A. Sanchez-Ruiz et al., "DC-Link Neutral Point Control for 3L-NPC Converters Utilizing Selective Harmonic Elimination - PWM," in IEEE Transactions on Industrial Electronics, vol. 69, no. 9, pp. 8633-8644, Sept. 2022, doi: 10.1109/TIE.2021.3113019.

DOI: https://doi.org/10.1109/TIE.2021.3113019

DC-Link Neutral Point Control for 3L-NPC Converters Utilizing Selective Harmonic Elimination – PWM

Alain Sanchez-Ruiz, *Senior Member, IEEE*, Mikel Mazuela, Hector Fernandez-Rebolleda, Salvador Ceballos, Angel Perez-Basante, Irati Ibanez-Hidalgo, Markel Zubiaga, Josep Pou, *Fellow, IEEE*, Neha Beniwal, *Student Member, IEEE*, Georgios Konstantinou, *Senior Member, IEEE*

***Abstract*—Selective harmonic elimination – pulsewidth modulation (SHE–PWM) is a modulation technique widely used to improve the efficiency and harmonic content in medium-voltage high-power converters. Among these converters, the three-level neutral-point-clamped (3L-NPC) converter is one of the most utilized topologies. However, the 3L-NPC converter requires a proper balancing of dc-link capacitor voltages. This paper presents a control technique, based on pulse shifting method, to regulate the neutral point voltage when SHE-PWM is utilized. The proposed technique performs well with any power factor and it can also be directly applied to T-type converters and easily extrapolated to other multilevel topologies. The proposed method is experimentally validated in a scaled-down power converter and a full-scale medium-voltage 3L-NPC converter.**

***Index Terms*— DC-link voltage control, modulation, neutral-point-clamped (NPC) converter, neutral-point control, selective harmonic elimination (SHE), voltage source converters (VSCs).**

I. INTRODUCTION

THE power ratings demanded in power-electronics-based applications are significantly increasing. In order to meet this challenge multilevel converters are a competitive solution. These converters are able to operate with higher power levels by increasing the application voltage instead of its current. This leads to higher efficiencies. In addition, better output power quality is achieved due to the increased number of levels in the output voltage [1]–[3]. Added to this, high power applications normally require high voltage semiconductors; for instance, insulated gate bipolar transistors (IGBT) or integrated gate-commutated semiconductors (IGCT) [4]. This medium voltage semiconductors are normally designed to have a good conduction behavior, while power losses are penalized. Due to this reason, the mentioned multilevel topologies need to be operated at low switching frequencies in order to increase their power density compared to low voltage solutions.

In multilevel converters, the dc-link neutral points or flying capacitor voltages need to be balanced, in addition to synthesizing the output voltage references [5]. Due to this fact, the modulation strategies originally developed for two-level power converters need to be modified. Pulsewidth modulation (PWM) [6] and space-vector modulation (SVM) [7]) are commonly used to operate the converter at high switching frequencies. Both of them present good dynamic response, but their performance worsens as the switching frequency decreases [2]. On the contrary, selective harmonic elimination (SHE-PWM) [8], [9] and its variants such as optimal pulse pattern (OPP) [10], [11] appear as attractive low–switching-frequency-based modulation techniques. SHE-PWM technique is based on offline calculation of transcendental equations that determine the switching instants of the converter in order to optimize the harmonic content of the output waveforms, which helps to increase the converter power density. Due to this reason, SHE-PWM is an attractive solution for high power multilevel converters.

One of the most widely used multilevel converter topology is the three-level neutral-point-clamped (3L-NPC) converter [12]. This topology is formed by two dc-link capacitors, building a neutral point, and the clamping diodes that connect the neutral point to the output terminals (see Fig. 1). In this topology, the neutral point balancing control is a major challenge. Many PWM or SVM techniques have been presented in the literature to overcome this issue; most of them are based on redundant switching states [7], [13]–[15]. However, extrapolating these methods to SHE-PWM is not straightforward since the switching frequency of the semiconductors may increase, which is not what is expected in a modulation type done to switch at low switching frequency [16]–[19]. The

Manuscript received January 19, 2021; revised April 27, 2021 and August 9, 2021; accepted August 30, 2021. This work was supported by the Basque Government within the research program ELKARTEK under the project CONVADP (KK-2020/00091)

Alain Sanchez-Ruiz and Markel Zubiaga are with Ingeteam R&D Europe, 48170 Zamudio, Spain (e-mail: alain.sanchez@ingeteam.com; markel.zubiaga@ingeteam.com).

Mikel Mazuela is with the Electronics and Computing Department, Mondragon Unibertsitatea, 20500 Mondragón, Spain (email: mmazuela@mondragon.edu).

Hector Fernandez-Rebolleda is with Ingeteam Power Technology, 48710 Zamudio, Spain (e-mail: hector.fernandez1@ingeteam.com).

Salvador Ceballos, Angel Perez-Basante and Irati Ibanez-Hidalgo are with Tecnalia, Basque Research and Technology Alliance, 48160 Derio, Spain (e-mail: salvador.ceballos@tecnalia.com; angel.perez@tecnalia.com; irati.ibanez@tecnalia.com).

Josep Pou and Neha Beniwal are with the School of Electrical and Electronic Engineering, Nanyang Technology University, Singapore 639798, Singapore (e-mail:josep.pou@ieee.org; neha006@e.ntu.edu.sg).

Georgios Konstantinou is with the School of Electrical Engineering and Telecommunications, University of New South Wales, Sydney, Sydney, NSW 2052, Australia (e-mail: g.konstantinou@unsw.edu.au).

neutral point balancing control with the commonly employed SHE-PWM, specially focused to three level converter topologies, has not been deeply analyzed in detail in the literature [16]–[26]. Other references [20], [22] use the self-balancing property of the 3L SHE-PWM applied in 3L-NPC converter; however, the neutral point regulation capability with distorted input ac-side current is not guaranteed. This self-balancing property is mainly fulfilled considering fundamental output current component. Some other references [23]–[26] propose switching angle displacement; however, these strategies lack of controllability under some power factors.

This paper presents a novel neutral point voltage balancing technique for SHE-PWM that is able to work correctly under any possible power factor condition, unlike previously published control methods associated with SHE-PWM. The proposed technique is based on pulse shifting method and is complemented with a band-limiting control to operate correctly under different reactive power demands. In this way, neutral point current formulation and analysis is served, and a comprehensive study of the capacitor voltage regulation under different active and reactive power conditions is accomplished. This solution can easily be extrapolated to any variants of 3L-NPC converter as three level active neutral point clamped (3L-ANPC) [1] or T-type [2] converters. To the authors knowledge, this is the first time that: 1) the capacitors voltages regulation is analyzed and analytically modeled in detail for a 3L-NPC converter with SHE-PWM; 2) capacitor voltages balancing solution is given based on pulse shifting for all the power factors and modulation index; for a 3L-NPC converter with SHE-PWM; 3) second harmonic distortion is identified and analyzed under pulse shifting method, giving a band-limiting controller solution to solve this issue.

The rest of this paper is organized as follows. The SHE-PWM formulation and resulting neutral point current is described in Section II. Section III presents the proposed technique to control dc-link capacitor voltages in a 3L-NPC converter, depending on the operating power factor. Section IV analyzes the proposed band-limiting control to improve the performance of the proposed balancing technique in the case the 3L NPC converter injects reactive power. Finally, experimental results obtained from two different converters, a down-scaled 3L-NPC converter prototype and a full-scale MV 3L-NPC converter, are shown in Section V.

II. Selective Harmonic Elimination for 3-Level Neutral Point Clamped Converter

Firstly, this section describes briefly the 3L-NPC topology and its associated switching states. In addition, the SHE-PWM formulation for 3L converters is also analyzed. Finally, the 3L-NPC neutral point balancing requirements are described.

A. 3L-NPC Converter Topology

The 3L-NPC converter topology, shown in Fig. 1, is widely utilized in the technical literature [12]. Each phase

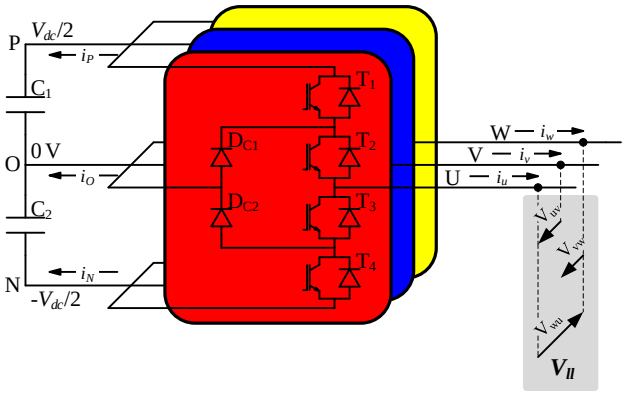

Fig. 1. 3L NPC converter topology scheme.

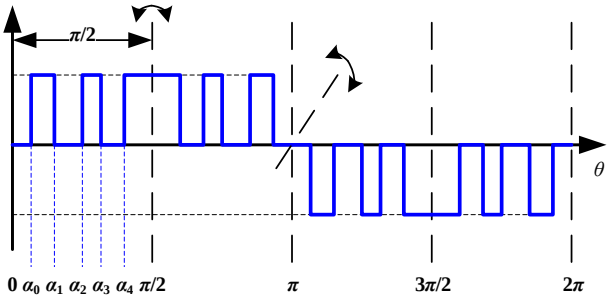

Fig. 2. 3L SHE5 generic waveform with QW symmetry in a fundamental period.

TABLE I
SWITCHING STATES OF 3L-NPC CONVERTER

T_1	T_2	T_3	T_4	V_{uO}	i_O
1	1	0	0	$V_{dc}/2$	-
0	1	1	0	0	$-i_u$
0	0	1	1	$-V_{dc}/2$	-

of the converter has four switching semiconductors (T_1..T_4), which contain their corresponding freewheeling diodes; furthermore, two clamping diodes (D_{C1}, D_{C2}) are also required.

The switching states of the topology are shown in Table I. As it can be observed, three different voltage levels can be achieved per phase with respect to the neutral point voltage of the dc-link, i.e., $V_{dc}/2$, 0 V and $-V_{dc}/2$.When one of the phases is clamped to the neutral point, the dc-link capacitor voltages become unbalanced because of the current that flows through the neutral point (i_O). Due to this fact, the modulation needs to fulfill two requirements:

- Reference voltage generation.
- DC-link capacitors voltage balancing.

B. Three-Level SHE-PWM

As the converter power increases and the voltage quality demand is higher, modulation techniques with low switching frequency, such as SHE-PWM [8], [9], [21] have gained relevance. SHE-PWM is generally based on the offline calculation of the switching angles in the first quarter wave (QW) of the phase output waveform, with the aim of controlling the fundamental voltage and eliminating undesired harmonics.

Classically, an SHE-PWM with N number of switching angles in the first QW has the following characteristics:

- The fundamental voltage is controlled to a

determined value, which depends on the modulation index:

$$\sum_{k=1}^{N} (-1)^{k+1} \cdot \cos(\alpha_k) = m_a \quad (1)$$

$$0 < \alpha_0 < \alpha_1 < .. < \alpha_{N-1} < \frac{\pi}{2} \quad (2)$$

$$m_a = \frac{\pi}{\sqrt{2}} \cdot \frac{V_{ph,1,rms}}{V_{dc}} \quad (3)$$

where α_k is the k number angle and m_a is the modulation index, if $V_{ph,1,rms}$ is the V_{u0} output fundamental rms voltage and V_{dc} is the total dc-link voltage. In addition, the firing angles are arranged in the order given by (2).

- The elimination of N-1 low-order odd nontriple harmonics are given by:

$$\sum_{k=1}^{N} (-1)^{k+1} \cdot \cos(n \cdot \alpha_k) = 0, \quad n = 5,7,11,13 \ldots \quad (4)$$

Fig. 2 shows a generic waveform of three-level SHE-PWM (3L SHE) shows an example of the whole fundamental period of 3L SHE5 waveform, where five firing angles are calculated in the first QW, henceforth called 3L SHE5. Thanks to QW symmetry, even harmonics are eliminated in the phase-neutral voltage (V_{ph}) and are not considered in (4). In a similar way, zero-sequence harmonics are neither considered in (4) due to their automatic elimination in the line-to-line voltages (V_{ll}) of three-phase systems.

Thanks to the symmetry of the positive and negative half-periods of the fundamental voltage waveform, even-order harmonics are eliminated in the converter phase voltage ($V_{ph} = V_{uO}$).

As a result, for a particular m_a range, different sets of firing angles can be found solving (1)-(4). These sets can be obtained through different calculation methods [8], [9], [21]. Once the solutions have been obtained, the phase output voltage waveforms for the rest of phases are obtained shifting the original waveform.

C. 3L-NPC Neutral Point Voltage Performance

The neutral point voltage at 3L-NPC converter is affected by the switching state selected for every phase (see possible switching states at Table I). Specifically, when the phase neutral voltage is clamped to 0 V, the phase current flows through the dc-link capacitors leading to a dc voltage unbalance. To simplify the analysis, the effect of each phase in the dc-link neutral point voltage can be analyzed independently. Afterwards, the superposition of the currents generated by every phase can be used to calculate the combined effect in the neutral point voltage. Accordingly, the average current through the neutral point by one of the phases can be expressed as:

$$\bar{I}_{ph-O} = \frac{1}{2\pi} \cdot \int_0^{2\pi} i_{ph-O}(\theta)\, d\theta \quad (5)$$

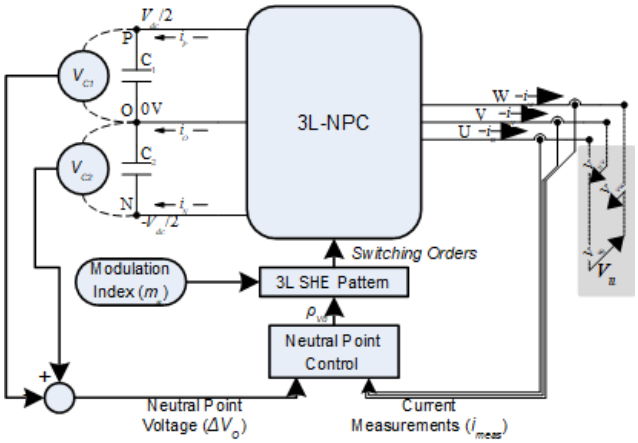

Fig. 3. Proposed modulation scheme.

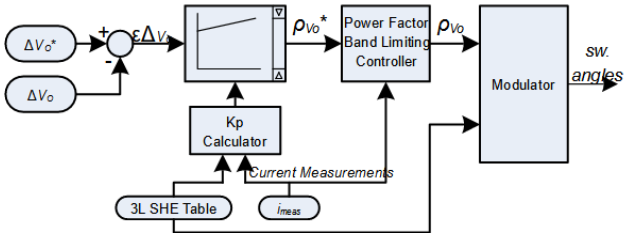

Fig. 4. Proposed neutral point control, where ΔVo is the measured neutral point voltage, ΔVo^* is the reference of the neutral point voltage (normally zero) and $\varepsilon\Delta Vo$ is the subtraction of reference and measurement

where,

$$i_{ph-O}(\theta) = \begin{cases} -i_{ph}, & V_{ph} = 0 \\ 0 & V_{ph} \neq 0 \end{cases} \quad (6)$$

Note that i_{ph} is the load current and can take instantaneous positive and negative values.

It can be demonstrated that the average value of the neutral point current provided by the SHE-PWM modulator is zero over a fundamental period. In this way, a theoretical natural balancing of the neutral point voltage is achieved. As there are three phases that influence on the neutral point voltage, a third harmonic component can be appreciated in the neutral point voltage ripple.

Nevertheless, despite this natural balancing property, the SHE-PWM modulator needs the capability to correct any unexpected dc-link neutral point voltage unbalance, which could be caused by several factors, such as distorted fundamental current, converter nonidealities, grid-side events or motor torque transients. In this way, with the aim of addressing this complex issue, which is additionally affected by the specific set of firing angles utilized by the modulator, a novel control is proposed in this work.

III. Proposed Neutral Point Voltage Control

This paper proposes a dc-link neutral point voltage control for 3L SHE applied to the 3L-NPC converter, considering different power factors. The main idea is the modification of the original sets of angles calculated to implement SHE-PWM with the aim of injecting a desired neutral point average current, with specific sign and amplitude, to balance the capacitor voltages.

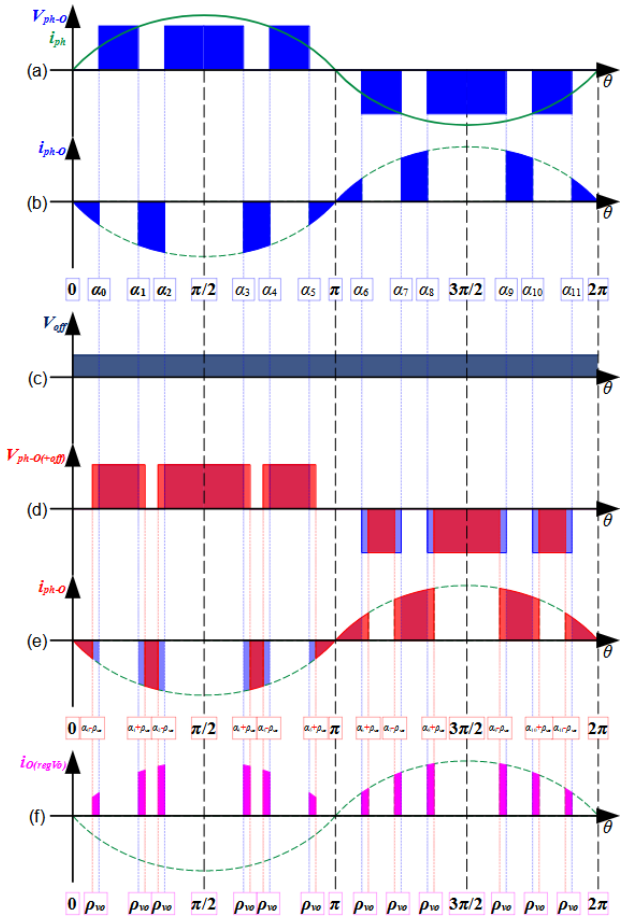

Fig. 5. Example of neutral point regulation with active power. (a) Theoretical 3L SHE3 phase voltage (blue) and phase current (green), (b) current through the neutral point (shaded in blue) due to one phase, (c) signal to be summed to the 3L SHE pattern to inject an average dc current in the neutral point, (d) modified 3L SHE pulse pattern with neutral point control, (e) modified current through the neutral point with neutral point control, and (f) neutral point current difference due to neutral point control.

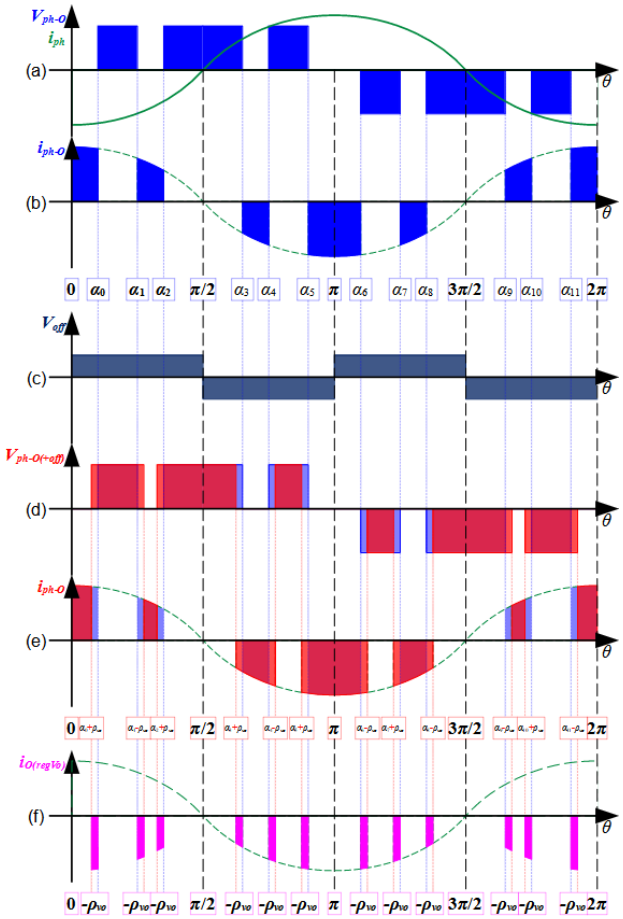

Fig. 6. Example of neutral point regulation with reactive power. (a) Theoretical 3L SHE3 phase voltage (blue) and phase current (green), (b) current through the neutral point (shaded in blue) due to one phase, (c) signal to be summed to the 3L SHE pattern to inject an average dc current in the neutral point, (d) modified 3L SHE pulse pattern with neutral point control, (e) modified current through the neutral point with neutral point control, and (f) neutral point current difference due to neutral point control.

In case a sinusoidal fundamental load current is considered, given by:

$$i_{ph} = i_u = I_{ph,max,1} \cdot \sin(\omega t - \varphi) \tag{7}$$

where $I_{ph,max,1}$ and φ are the amplitude and phase difference with respect to phase voltage, respectively, the average current through the neutral point generated by one phase can be formulated as the sum of the currents applied to the neutral point throughout the fundamental period by that phase. As it has been commented previously, these currents are injected when the phase-neutral voltage is 0 V:

$$\begin{aligned}\bar{I}_{ph-O} &= \frac{1}{2\pi} \cdot \left[\int_{0}^{\alpha_0-\rho_{Vo}} -i_{ph}(\theta)d\theta + \ldots + \int_{\alpha_{(N-2)}+\rho_{Vo}}^{\alpha_{(N-1)}-\rho_{Vo}} -i_{ph}(\theta)d\theta \right. \\ &+ \int_{\alpha_{N}-\rho_{Vo}}^{\alpha_{(N-1)}+\rho_{Vo}} -i_{ph}(\theta)d\theta + \ldots + \int_{\alpha_{(2N-1)}-\rho_{Vo}}^{\pi} -i_{ph}(\theta)d\theta \\ &+ \int_{\pi}^{\alpha_{(2N)}+\rho_{Vo}} -i_{ph}(\theta)d\theta + \ldots + \int_{\alpha_{(3N-2)}-\rho_{Vo}}^{\alpha_{(3N-1)}+\rho_{Vo}} -i_{ph}(\theta)d\theta \\ &+ \left. \int_{\alpha_{(3N)}+\rho_{Vo}}^{\alpha_{(3N+1)}-\rho_{Vo}} -i_{ph}(\theta)d\theta + \ldots + \int_{\alpha_{(4N-1)}+\rho_{Vo}}^{2\pi} -i_{ph}(\theta)d\theta \right]\end{aligned} \tag{8}$$

where ρ_{Vo} is a possible switching angle variation introduced by the modulator with respect to the original set of angles calculated by an offline method. If ρ_{Vo} is equal to zero, the natural balancing capability of the 3L NPC theoretically provides a null average value of the $I_{ph\text{-}O}$. On the contrary, if $\rho_{Vo} \neq 0$, a neutral point current with an average value given by (8) will be injected.

This angle shift (ρ_{Vo}) is an additional degree of freedom that can be exploited by the neutral point voltage controller. The way to calculate the optimum ρ_{Vo} will depend on the power factor.

The proposed modulation scheme block diagram is shown in Fig. 3. As it can be observed, besides the three phase currents, the voltages of both dc-link capacitors are required as input measurements to the proposed neutral point voltage controller. Based on these measurements, the controller calculates the necessary ρ_{Vo} per switching angle to inject the required average neutral point current for balancing the dc-link voltage. This is added to the 3L SHE pattern and applied as real switching orders.

A general scheme of the neutral point voltage controller is illustrated in Fig. 4. As it can be noticed, ρ_{Vo}^* is calculated by means of an adaptive proportional-integrative (PI) controller whose tuning will depend on the power factor as it will be described in next subsections. The resultant switching angle shift (ρ_{Vo}) is the result of the combination of the methods proposed for active and reactive power strategies. In case the converter injects reactive power, a band limiting controller, whose design is discussed in section IV, is utilized to improve the performance of the proposed neutral point voltage controller.

A. Active Power Regulation

The idea in which the proposed controller relies in case of active power loads is to use ρ_{Vo} to create a zero-sequence dc voltage component that is added to the phase voltage. By doing this, the generated neutral point current is modified accordingly. The operation behind this idea is illustrated in Fig. 5 for a 3L SHE3 (three calculated firing angles in the first QW). In Fig. 5(a), the theoretical 3L SHE3 phase voltage and the phase current when ρ_{Vo}=0, are depicted. Fig. 5(b) shows in blue color the current through the neutral point of the dc-link generated by one of the phases. Alternatively, Fig. 5(c) shows the desired dc zero-sequence voltage that is added to the SHE pattern by introducing a ρ_{Vo} phase shift. Fig. 5(d) shows the way ρ_{Vo} is applied and how it modifies the 3L SHE3 voltage pattern, while Fig. 5(e) shows the generated neutral point current. The last signal in magenta shows the current difference introduced due to the phase shift ρ_{Vo}. It can be stated that average value of the current through the neutral point is not zero thanks to the use of ρ_{Vo}.

Using (8), the average current through the neutral point created by the three phases for N firing angles in the first QW when ρ_{Vo} is used can be analytically expressed as:

$$\bar{I}_O \approx \frac{6}{\pi} \cdot I_{ph,max,1} \cdot \rho_{Vo} \cdot \sum_{k=0}^{N-1} \sin(\alpha_k) = I_{ph,rms,1} \cdot \rho_{Vo} \cdot K_{o,P} \quad (9)$$

where $K_{o,P}$ is the gain of the adaptive PI controller in Fig. 4. As it can be noticed, $K_{o,P}$ is directly dependent on the utilized set of angles. Its value is given by:

$$K_{o,P} = \frac{6}{\pi} \cdot \sum_{k=0}^{N-1} \sin(\alpha_k) \quad (10)$$

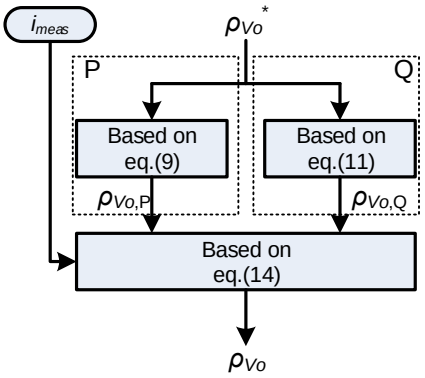

Fig. 7. Decoupling of ρ_{Vo} depending on the power factor. ρ_{Vo}^* represents reference value from controller and ρ_{Vo} the applied phase shift.

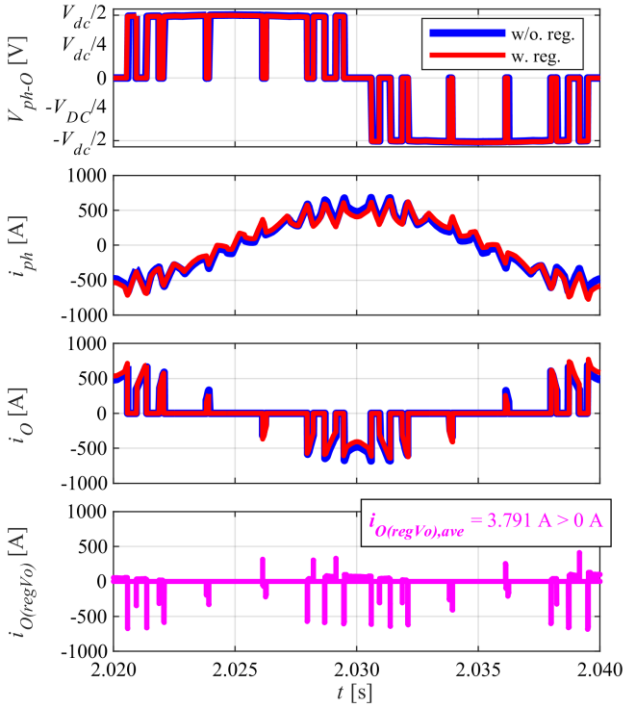

Fig. 8. Effect of the distortion created by the second harmonic injection. (a) Phase voltage (V_{ph}), (b) phase current (i_{ph}), (c) current through the neutral point created by one phase, and (d) neutral point current difference due to neutral point control voltage.

Thus, having dc-link capacitor voltage error as the input of the PI controller, the resultant pulse shift in the only active power case would be $\rho_{Vo}^* = \rho_{Vo,P} = \rho_{Vo}$.

B. Reactive Power Regulation

In case the 3L-NPC converter injects reactive power, the scenario is illustrated in Fig. 6. This graph shows the waveforms when the current is 90º lagging the voltage, but this strategy can also be applied when the current is 90º leading.

In this case, due to symmetry between the phase voltage and current, ρ_{Vo} needs to be calculated to inject a second harmonic in the phase-neutral voltage. Consequently, the voltage pattern is modified by ρ_{Vo} as indicated in Fig. 6(c). Hence, thanks to this second harmonic, an average current in the neutral point is accomplished and its required sign is obtained adjusting the phase of the second harmonic.

:

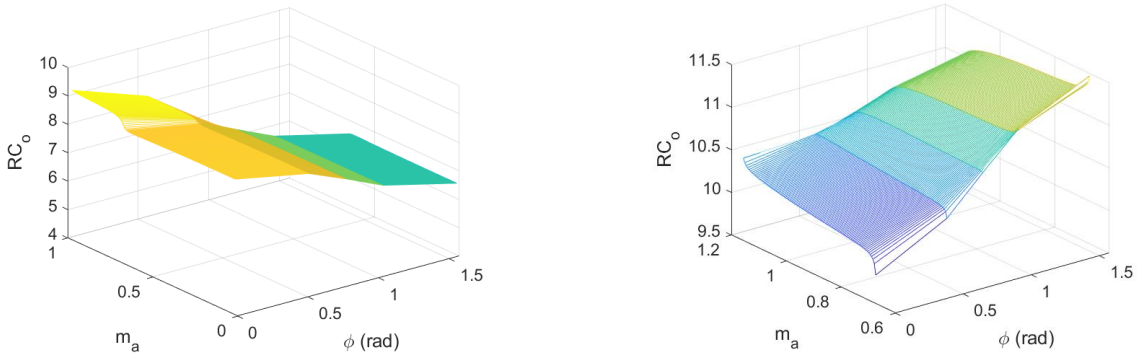

Fig. 9. Neutral point regulation capability for different modulation index and power factor points. (a) 3L SHE6 and (b) 3L SHE9.

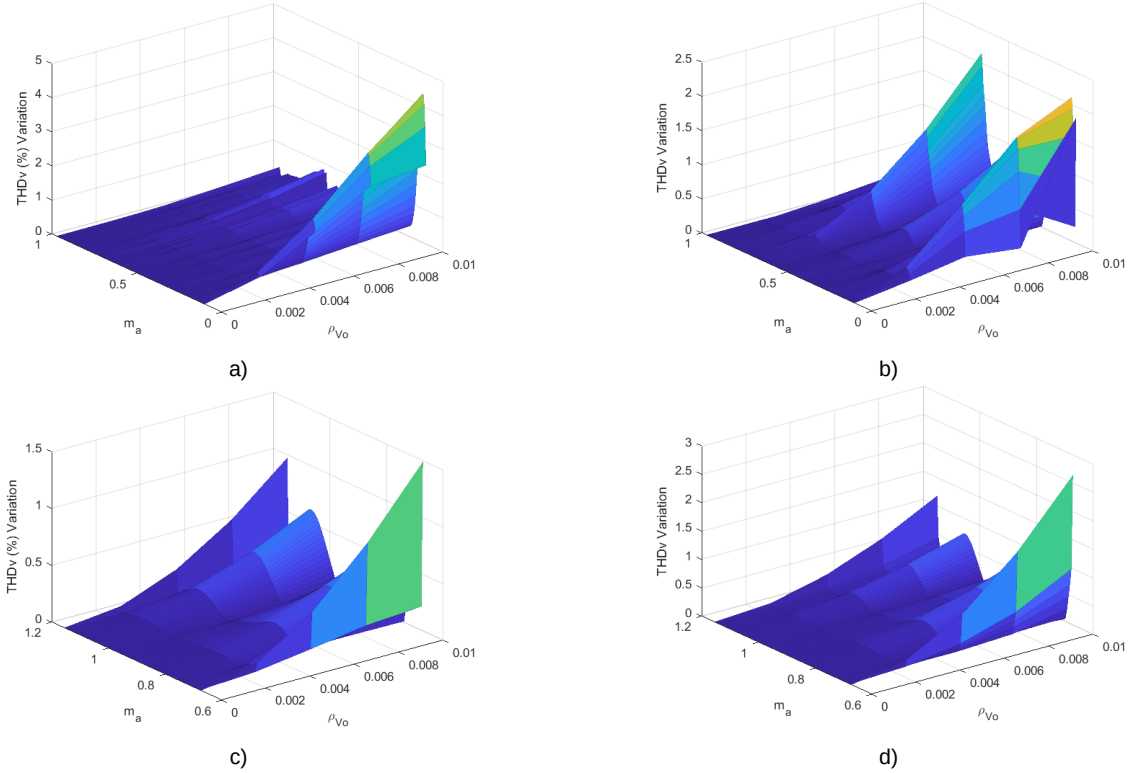

Fig. 10. Voltage THD variation due to phase shift (ρ_{Vo}), depending on modulation index.(m_a). (a) 3L SHE6 with completely active power, (b) 3L SHE6 with completely reactive power, (c) 3L SHE9 with completely active power, (d) 3L SHE9 with completely reactive power.

Using (8), the average current through the neutral point is given by

$$\bar{I}_O \approx -\frac{6}{\pi} \cdot I_{ph,max,1} \cdot \rho_{Vo} \cdot \sum_{k=0}^{N-1} \cos(\alpha_k) = \\ = I_{ph,rms,1} \cdot \rho_{Vo} \cdot K_{o,Q} \quad (11)$$

where $K_{o,Q}$ is the PI gain associated to the set of angles selected to implement SHE-PWM:

$$K_{o,Q} = -\frac{6}{\pi} \cdot \sum_{k=0}^{N-1} \cos(\alpha_k) \quad (12)$$

Thus, having dc-link capacitor voltage error as the input of the PI controller, the resultant pulse shift in the only reactive power case would be $\rho_{Vo}^* = \rho_{Vo,Q} = \rho_{Vo}$.

Finally, it is important to highlight that in this case, due to the second harmonic, the converter phase output currents will be distorted. This is a method already introduced in classical carrier based PWM modulation [27] and it is assumed to under the grid codes if its amplitude is small. Thus, the neutral point current will also be affected by this distortion, and the limiting-band control proposed in

Section IV should be used to cancel out the neutral point voltage deviations properly.

C. Combination of Active and Reactive Power

Although active (P) and reactive (Q) power cases have been separately analyzed in Sections III.A and 0, most common scenarios will normally demand both, P and Q. Hence, the applied ρ_{Vo} per switching angle will be the result of a combination of the calculation techniques designed for both power modes. In this way, this combination is implemented applying weighting factors to (9) and (11), resulting in:

$$\bar{I}_O \approx I_{ph,rms,1} \cdot \rho_{Vo} \cdot \left((\cos(\varphi))^2 \cdot K_{o,P} + (\sin(\varphi))^2 \cdot K_{o,Q}\right) \quad (13)$$

where φ is the phase difference between phase voltage and current.

Regarding (13), the ρ_{Vo} per switching angle is obtained decoupling the calculations associated to P and Q. Depending on the power factor, the displacement angles of P ($\rho_{Vo,P}$) and Q ($\rho_{Vo,Q}$) are combined through weighting factors:

$$\rho_{Vo} = (\cos\varphi)^2 \cdot \rho_{Vo,P} + (\sin\varphi)^2 \cdot \rho_{Vo,Q} \quad (14)$$

Therefore, the Power Factor Controller block of Fig. 4 can be ideally simplified as in Fig. 7. As a result, an average neutral point current with the required amplitude and sign to balance the neutral point voltage will be obtained for any power factor condition.

In order to evaluate the capability of regulating the neutral point in all power factors or modulation index, indicator RC_o is defined as follows.

$$RC_o = \frac{6}{\pi} \cdot \sqrt{RC_{o,Q}{}^2 + RC_{o,P}{}^2} \quad (15)$$

where,

$$RC_{o,Q} = sin(\varphi) \cdot \sum_{k=0}^{N-1} \cos(\alpha_k) \quad (16)$$

$$RC_{o,P} = cos(\varphi) \sum_{k=0}^{N-1} \sin(\alpha_k) \quad (17)$$

These variables represent the amount of current flowing to the neutral point depending on how long the output voltage clamped to 0 V and the current value (due to power factor) in that time gap.

Each angle set is evaluated using equation (15) for each modulation index and power factor. The results obtained are shown in Fig. 9 for 3L SHE6 (3L SHE with six calculated angles per quarter waveform) and 3L SHE9 (3L SHE with nine calculated angles per quarter waveform) switching angle sets which are used in experimental results. It is important to have no modulation index and power factor point close to zero, which would mean having no neutral point control capability, rather than the RC_o value.

Analyzing the results in Fig. 9 achieved both analyzed switching tables obtain quite constant regulation capability, no matter which modulation index or power factor the proposed algorithm is working. As it can be appreciated, the used angle set is extremely dependent on the neutral point regulation capability. Even for the same number of angles, there can be clear differences in the neutral point regulation capability.

Apart from the neutral point regulation, the minimum space between two consecutive switching angles does have a high impact in the capability of regulating the neutral point. As two consecutive switching angles cannot be overlapped, this is the maximum ρ_{Vo} that needs to be allowed to the control proposed in Fig. 7.

It needs to be said that, as the original SHE-PWM angles are modified, the output voltage waveform will be slightly

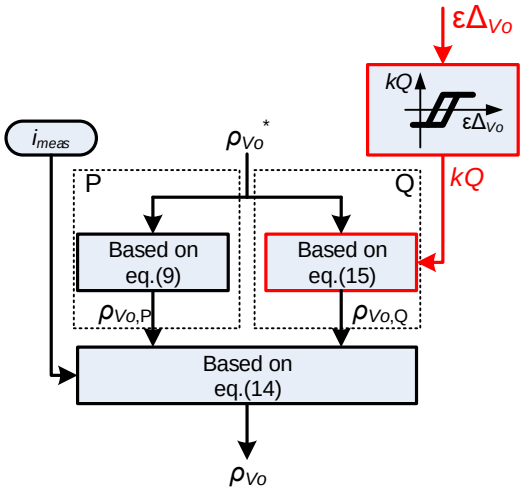

Fig. 11. Decoupling of ρ_{Vo} depending on the power factor with the proposed band-limiting controller (in red).

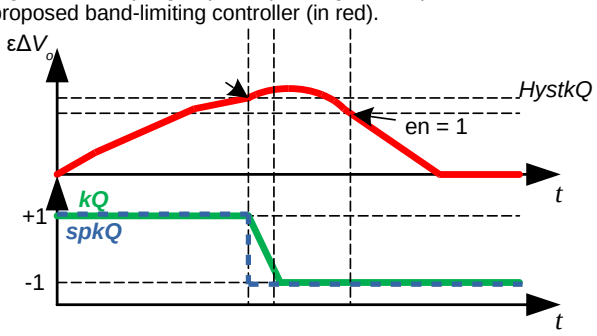

Fig. 12. Proposed band-limiting controller example.

distorted. Fig. 10 shows the THD increase for the 3L SHE6 and 3L SHE9 angle sets for the cases where the converter is only working with active power or reactive power. In a normal operating mode, the applied effective phase-shift should be around 0rad. This should not be a problem with active power operation. However, with reactive power operation a transient to the maximum could happen. Due to this reason, a proper selection of the used angle set and the fact that the applied angle-shifting needs to be small (<0.01rad) minimizes this phenomenon, achieving acceptable harmonic performance.

IV. Band-Limiting Control for Reactive Power Operation

As it has been analyzed in Section III, the injection of a second harmonic in the phase neutral voltage is required in order to balance the neutral point voltage, in case the 3L-NPC converter injects reactive power. However, this negative sequence harmonic distorts the phase output currents.

Furthermore, in order to calculate the sign of the average neutral point current, only the fundamental harmonic is considered. This assumption is closer to reality as the number of eliminated harmonics in the original SHE-PWM pattern is higher. However, the distortion introduced by the second harmonic in the current waveform injected in the neutral point, can make the neutral point control not to work properly. This effect can be seen in Fig. 8, where the output phase voltage, output current, neutral point current and

Fig. 13. Scaled-down 3L-NPC converter.

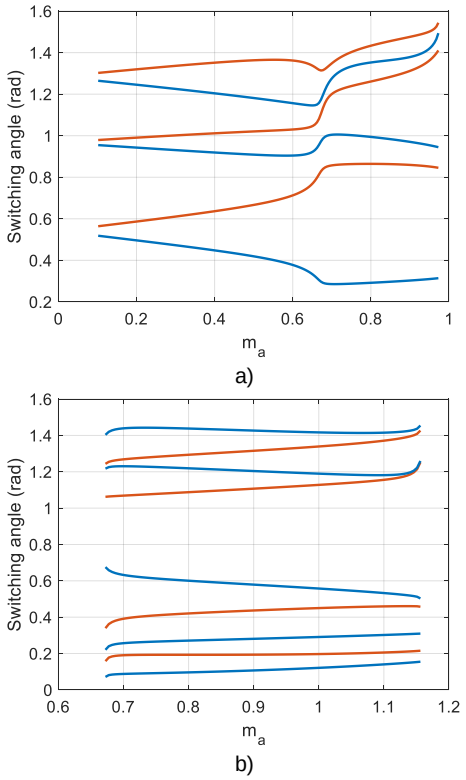

Fig. 14. Used experimental angle sets. Blue or red meaning positive or negative voltage step, respectively. a) 3L SHE6 and b) 3L SHE9.

TABLE II
EXPERIMENTAL DATA. SCALED-DOWN POWER CONVERTER

DC-link voltage	430V
DC-link semibus capacitance	1.65mF
AC maximum voltage	263V
Motor nominal power	75kW

TABLE III
EXPERIMENTAL DATA. FULL SCALE MV POWER CONVERTER

DC-link voltage	6400V
DC-link semibus capacitance	2mF
AC maximum voltage	4160V
Motor nominal power	4MW

current difference in the neutral point with and without neutral point control are shown. It can be seen how the phase shift is introduced to create a negative average value, but the distortion of the current creates a positive average current. This can make the neutral point regulator decide wrongly the phase of the second harmonic injected with ρ_{Vo}.

Therefore, as the system is required to operate across a range of SHE-PWM firing angles, dc-link capacitor voltages and output current, a band-limiting control is proposed. This control only affects the phase of the injected second harmonic when working with reactive power.

With this purpose, a variable *kQ* is defined to determine the sign of the second harmonic for reactive power operation. Equation (11) is modified as follows:

$$\bar{I}_O \approx -\frac{6}{\pi}\cdot I_{ph,max,1}\cdot kQ\cdot \rho_{Vo}\cdot \sum_{k=0}^{N-1}\cos(\alpha_k) = \\ = I_{ph,rms,1}\cdot kQ\cdot \rho_{Vo}\cdot K_{o,Q} \quad (18)$$

where $kQ \in [-1,1]$. While *kQ* can take any value from -1 to 1, it should always be operating in the limits. $kQ = 1$ means that the second harmonic is injected with the theoretical phase, while $kQ = -1$ means that the band-limiting controller is acting and the second harmonic is injected with 180º phase shift with respect to the theoretical phase.

Using the proposed technique, the sign of the injected second harmonic is changed depending on the unbalance in the capacitor voltages, instead of depending on the power factor. Hence, the uncertainty introduced by the second harmonic sign is eliminated in this way. Therefore, the schematic block of the ρ_{Vo} decoupling shown in Fig. 7 is transformed as it is depicted in Fig. 11.

Fig. 12 illustrates an implementation example of the proposed technique. In this figure, the error of the dc-link capacitors voltages ($\varepsilon\Delta V_o$) is compared to a parameter *HystkQ*, which is the maximum allowable neutral point deviation to assume that the band-limiting controller needs to act. The speed to reach the *HystkQ* value will depend on the maximum allowable ρ_{Vo}; a trade-off between dynamics and output voltage distortion needs to be done (see Fig. 10). Once the divergence between both dc-link capacitor voltages exceeds the maximum threshold, the band-limiting control changes the *kQ* value to obtain the reference *spkQ*.

While *spkQ* toggles from 1 to -1, or viceversa, *kQ* is ramped so the second harmonic amplitude crosses zero smoothly. As it can be noticed, the proposed band-limiting controller only acts changing the sign of the second harmonic with reactive power.

In order to make the proposed method work, the angle set selection is a key factor, as highlighted previously. The value of *HystkQ* is also relevant. The selected *HystkQ* value is the voltage value where the decision made in the neutral point voltage regulation is considered to be wrong, so the *spkQ* value toggles. This value should be selected to be not too low so any dynamic response does not make *spkQ* react; but not too high so the neutral point regulation is completely lost.

V. EXPERIMENTAL RESULTS

The proposed technique is experimentally validated using two different power converters: a scaled-down prototype and a full-scale converter.

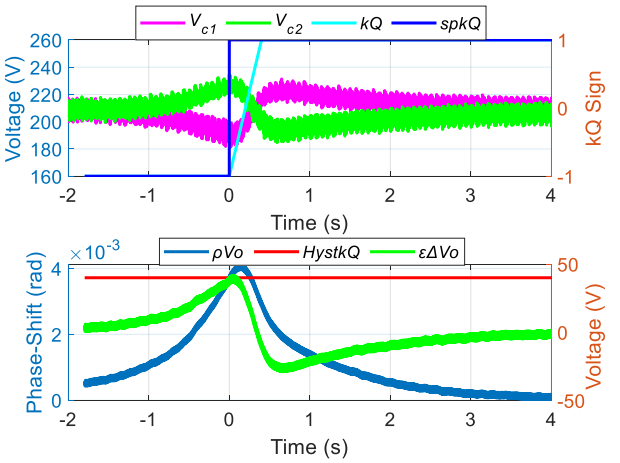

Fig. 15. Capacitor voltages with band-limiting control actuation as the output Q decreases. 3L SHE6, *fo* = 25Hz, ΔV_o^* = 0V. (a) Capacitor voltages 1 and 2 and *kQ* and *spkQ* signals and (b) neutral point voltage error ($\varepsilon\Delta V_o$) and phase-shift angle (ρV_o).

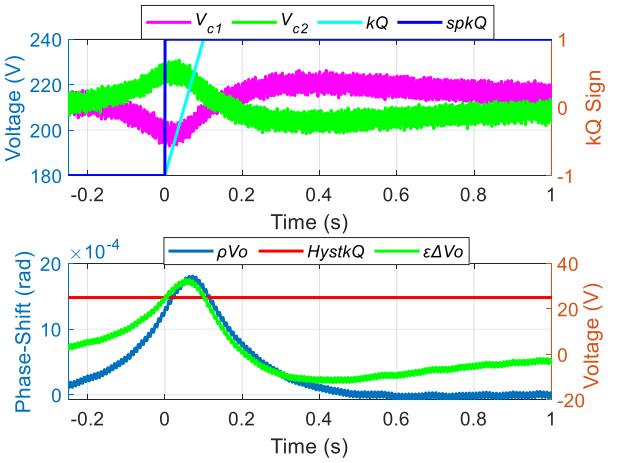

Fig. 16. Capacitor voltages with band-limiting control actuation as the output Q decreases. 3L SHE9, *fo* = 25Hz, ΔV_o^* = 0V. (a) Capacitor voltages 1 and 2 and *kQ* and *spkQ* signals and (b) neutral point voltage error ($\varepsilon\Delta V_o$) and phase-shift angle (ρV_o).

A. Scaled-Down 3L-NPC Converter

Firstly, a scaled-down 3L-NPC power converter (see Fig. 13) is used, which is placed at the Power Electronics Laboratory of Ingeteam Power Technology. The dc voltage is generated by a 12-pulse rectifier, that produces 460Vdc. The maximum achievable output voltage fundamental is 263Vac,rms. A 75-kW induction motor with no load is connected to the output terminals. Voltage/frequency open-loop regulation is used. In this way, the converter works with inductive power, which is the problematic operating point identified in this work and any control issue (apart from neutral point regulation) is avoided. As no load is connected to the motor, only magnetizing current flows from the converter. A summary of the experimental setup parameters is provided in Table II. Added to this, used angle sets are depicted in Fig. 14, where evolution of 3L SHE6 and 3L SHE9 with the modulation index can be appreciated.

Two main cases are tested with this layout. In the first case, the converter works with a fundamental frequency of f_o = 25Hz and a 3L SHE6 (a set of firing angles to implement SHE-PWM for a three-level converter with six

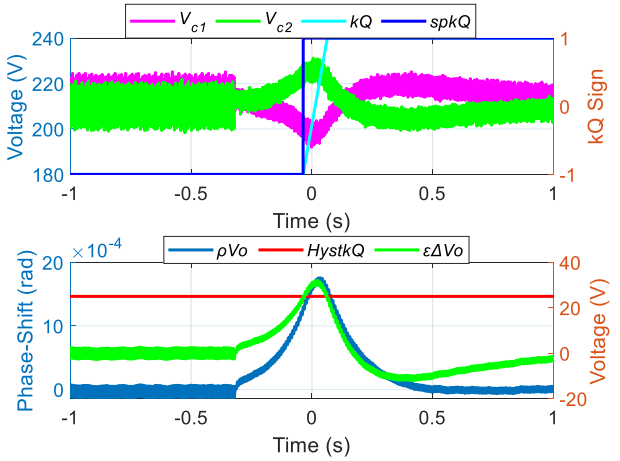

Fig. 17. Capacitor voltages with band-limiting control actuation as the output Q decreases. 3L SHE6 to 3L SHE9, *fo* = 25Hz, ΔV_o^* = 10V. (a) Capacitor voltages 1 and 2 and *kQ* and *spkQ* signals and (b) neutral point voltage error ($\varepsilon\Delta Vo$) and phase-shift angle (ρVo).

angles in the first QW, applying QW symmetry). With these conditions, the reactive power is gradually decreased, until the second harmonic injection distortion has a big impact and its sign needs to be changed with the band-limiting control. This can be seen in Fig. 15. As it can be observed, once the capacitor voltages start diverging and exceed the voltage limit, the second harmonic sign is changed (*spkQ* represents the reference, and *kQ* the effective harmonic change).

The same test case is presented in Fig. 16, but applying a 3L SHE9 set of angles, with nine firing angles in the first QW. This test is done for an operating point with a higher Q value. The same effect than using 3L SHE6 can be appreciated. It can also be concluded that the Q level in order to need a second harmonic change is dependent on the SHE angle set, but the method is effective whichever the angle set is.

Fig. 17 shows a case where the power converter initially works using the 3L SHE6 angle set and afterwards changes to 3L SHE9 angle set. In this case, the ΔVo^* reference is set to 10V. The change instant can be appreciated in when the capacitor voltage ripple suddenly changes. The set 3L SHE9 is not able to properly regulate the neutral point voltage due to the second harmonic distortion. Due to this reason, the limiting-band control changes the second harmonic sign, providing the ability to regulate the neutral point voltage.

B. Full-Scale MV Converter

The proposed algorithm is programmed in a 4.16kV, 4MW Ingedrive MV100 power converter connected to a power grid. It has a back-to-back configuration, feeding a motor. The converter under analysis is the grid-side converter. The objective of these tests is to validate the performance of the proposed method when working simultaneously with active and reactive power, using different capacitor voltage error references. The characteristics of the converter are summarized in Table III.

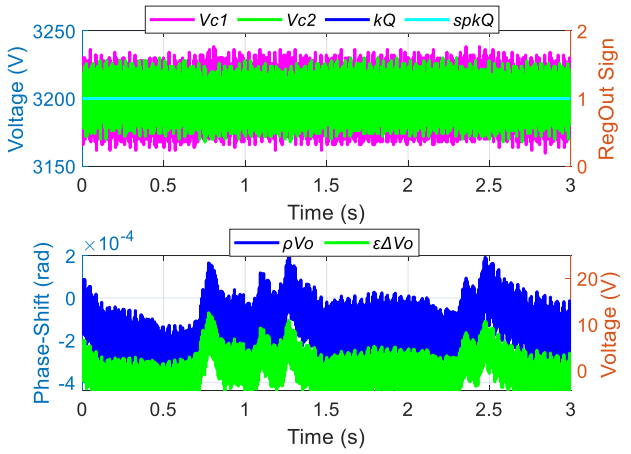

Fig. 18. Capacitor voltages with 204A, power factor of 0.34 and $\Delta V_o^* = 0$V. (a) Capacitor voltages 1 and 2 and *kQ* and *spkQ* signals and (b) neutral point voltage error ($\varepsilon\Delta V_o$) and phase-shift angle (ρV_o).

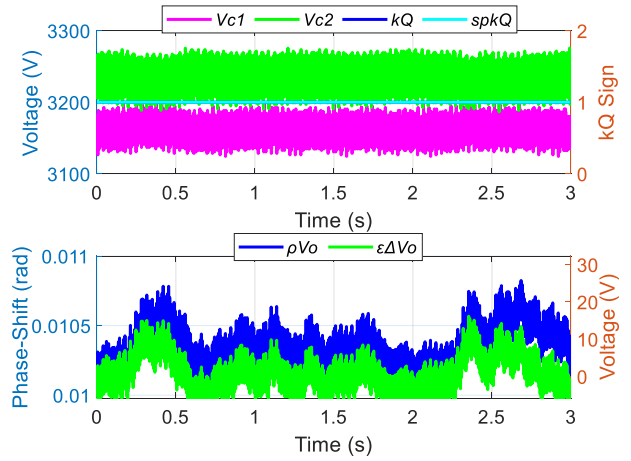

Fig. 19. Capacitor voltages with 204A, power factor of 0.34 and $\Delta V_o^* = 75$V. (a) Capacitor voltages 1 and 2 and *kQ* and *spkQ* signals and (b) neutral point voltage error ($\varepsilon\Delta V_o$) and phase-shift angle (ρV_o).

Fig. 18 and Fig. 19 show the dc-link capacitor voltages working with a power factor of 0.34, a phase current of 204A and a reference error $\varepsilon\Delta V_O$ of 0V and 75V, respectively. In both cases, the proposed control operates correctly. The lower subplot of both figures shows the voltage error (in green) with respect to the error reference. Hence, as both converge to 0V, this means that Fig. 18 reaches 0V, and Fig. 19 75V error. In this way the regulation capability of the proposed method is demonstrated. As the active power has some influence, the band-limiting control is not required to be activated.

All these carried out experimental tests demonstrate the suitability of the proposed method in different conditions:

- Experimental results with different angle sets are carried out with 3L SHE6 and 3L SHE9 in Fig. 15 and Fig. 16, respectively. In this way, when the angle set is different, the asked ρV_o is also different. The method is in the same way effective.
- Transition of both switching angle sets is made in Fig. 17. As the number of angles is different, the current value where the generated second order current harmonic generates the neutral point average error is different. Thus, for the same output current value a transition from 3L SHE6 to 3L SHE9 generates the band-limiting controller actuation.
- Finally, active power neutral point correction is also tested in a real MV converter. The neutral point error setpoint is set to 0V (in Fig. 18) and 75V (in Fig. 19). The proposed algorithm behaves properly.

All these tests demonstrate the suitability of the proposed analysis for different scenarios.

VI. Conclusion

A novel method to balance the neutral point voltage in 3L-NPC converters has been proposed to be applied along with SHE-PWM. The proposed method is based on a phase shift of original firing angles, given by SHE-PWM calculation, to inject the desired neutral point current. The method works well for any power factor conditions. Depending on the power factor, a dc voltage component or second order harmonic are added to the voltage reference, when working with active or reactive power, respectively. However, adding a second order harmonic has a direct impact in the phase output current distortion. In order to overcome the problems that the second harmonic generates in the dc-link neutral point voltage control, a band-limiting controller has also been proposed.

The proposed method has been analytically described and experimentally validated in a scaled-down 3L-NPC converter and also in a full-scale MV 3L-NPC converter.

The proposed balancing technique can also be directly applied to T-type converters and easily extrapolated to any multilevel topology.

References

[1] S. Kouro, M. Malinowski, K. Gopakumar, J. Pou, L. G. Franquelo, Bin Wu, J. Rodriguez, M. A. Perez, and J. I. Leon, "Recent advances and industrial applications of multilevel converters," *IEEE Trans. Ind. Electron.*, vol. 57, no. 8, pp. 2553–2580, Aug. 2010.

[2] A. Sanchez-Ruiz, M. Mazuela, S. Alvarez, G. Abad, and I. Baraia, "Medium voltage–high power converter topologies comparison procedure, for a 6.6 kV drive application using 4.5 kV IGBT modules," *IEEE Trans. Ind. Electron.*, vol. 59, no. 3, pp. 1462–1476, Mar. 2012.

[3] A. Sanchez-Ruiz, J. J. Valera-García, I. Legarra, I. Torre, S. Telleria, and I. Atutxa, "Modeling of MVDC Multidrive Systems for Power Quality Analysis," *IEEE Trans. Ind. Electron.*, vol. 68, no. 7, pp. 5507–5516, Jul. 2021.

[4] F. Filsecker, R. Alvarez, and S. Bernet, "Comparison of 4.5-kV press-pack IGBTs and IGCTs for medium-voltage converters," *IEEE Trans. Ind. Electron.*, vol. 60, no. 2, pp. 440–449, Feb. 2013.

[5] J. I. Leon, S. Kouro, L. G. Franquelo, J. Rodriguez, and B. Wu, "The essential role and the continuous evolution of modulation techniques for voltage-source inverters in the past, present, and future power electronics," *IEEE Trans. Ind. Electron.*, vol. 63, no. 5, pp. 2688–2701, May 2016.

[6] J. Holtz, "Pulsewidth modulation for electronic power conversion," *Proc. IEEE*, vol. 82, no. 8, pp. 1194–1214, Aug. 1994.

[7] J. Pou, R. Pindado, D. Boroyevich, and P. Rodriguez, "Limits of the neutral-point balance in back-to-back-connected three-level

converters," *IEEE Trans. Power Electron.*, vol. 19, no. 3, pp. 722–731, May 2004.
[8] M. S. A. Dahidah, G. Konstantinou, and V. G. Agelidis, "A review of multilevel selective harmonic elimination PWM: formulations, solving algorithms, implementation and applications," *IEEE Trans. Power Electron.*, vol. 30, no. 8, pp. 4091–4106, Aug. 2015.
[9] A. Perez-Basante, S. Ceballos, G. Konstantinou, J. Pou, I. Kortabarria, and I. M. de Alegría, "A universal formulation for multilevel selective-harmonic-eliminated PWM with half-wave symmetry," *IEEE Trans. Power Electron.*, vol. 34, no. 1, pp. 943–957, Jan. 2019.
[10] A. K. Rathore, J. Holtz, and T. Boller, "Synchronous optimal pulsewidth modulation for low-switching-frequency control of medium-voltage multilevel inverters," *IEEE Trans. Ind. Electron.*, vol. 57, no. 7, pp. 2374–2381, Jul. 2010.
[11] V. Spudić and T. Geyer, "Model predictive control based on optimized pulse patterns for modular multilevel converter STATCOM," *IEEE Trans. Ind. Appl.*, vol. 55, no. 6, pp. 6137–6149, Nov. 2019.
[12] A. Nabae, I. Takahashi, and H. Akagi, "A New Neutral-Point-Clamped PWM Inverter," *IEEE Trans. Ind. Appl.*, vol. IA-17, no. 5, pp. 518–523, Sep. 1981.
[13] J. Shen, S. Schroder, B. Duro, and R. Roesner, "A neutral-point balancing controller for a three-level inverter with full power-factor range and low distortion," *IEEE Trans. Ind. Appl.*, vol. 49, no. 1, pp. 138–148, Feb. 2013.
[14] G. Zhang, B. Wei, X. Gu, X. Li, Z. Zhou, and W. Chen, "Sector subdivision based SVPWM strategy of neutral-point-clamped three-level inverter for current ripple reduction," *Energies*, vol. 12, no. 14, p. 2734, Jul. 2019.
[15] M. Wu, Y. Li, and G. Konstantinou, "A comprehensive review of capacitor voltage balancing strategies for multilevel converters under selective harmonic elimination PWM," *IEEE Trans. Power Electron.*, pp. 1–1, 2020.
[16] K. Imarazene, H. Chekireb, and E. M. Berkouk, "Balancing DC link using the redundant states method in selective harmonics elimination PWM," in *8th International Symposium on Advanced Electromechanical Motion Systems Electric Drives Joint Symposium*, Jul. 2009, pp. 1–5.
[17] Tongsheng Zhang, Chunshui Du, Changwei Qin, Xiangyang Xing, Alian Chen, and Chenghui Zhang, "Neutral-point voltage balancing control for three-level T-type inverter using SHEPWM," in *IEEE 8th International Power Electronics and Motion Control Conference (IPEMC-ECCE Asia)*, May 2016, pp. 1116–1122.
[18] C. Hu, G. Holmes, W. Shen, X. Yu, Q. Wang, and F. Luo, "Neutral-point potential balancing control strategy of three-level active NPC inverter based on SHEPWM," *IET Power Electron.*, vol. 10, no. 14, pp. 1943-1950(7), Nov. 2017.
[19] S. R. Pulikanti, M. S. A. Dahidah, and V. G. Agelidis, "SHE-PWM switching strategies for active neutral point clamped multilevel converters," in *2008 Australasian Universities Power Engineering Conference*, Dec. 2008, pp. 1–7.
[20] K. Imarazene, E. M. Berkouk, and H. Chekireb, "Selective harmonics elimination PWM with sel-balancing capacitors in three-level inverter," in *6th IET International Conference on Power Electronics, Machines and Drives (PEMD)*, Mar. 2012, pp. 1–6.
[21] A. Sanchez-Ruiz, G. Abad, I. Echeverria, I. Torre, and I. Atutxa, "Continuous phase-shifted selective harmonic elimination and DC-link voltage balance solution for H-bridge multilevel configurations, applied to 5L HNPC," *IEEE Trans. Power Electron.*, vol. 32, no. 4, pp. 2533–2545, Apr. 2017.
[22] K. Imarazene, E. M. Berkouk, and H. Chekireb, "Self-balancing DC-link capacitor voltages in seven-level inverter using selective harmonics elimination PWM," in *IEEE 11th Conference on Industrial Electronics and Applications (ICIEA)*, Jun. 2016, pp. 922–927.
[23] S. R. Pulikanti, M. S. A. Dahidah, and V. G. Agelidis, "Voltage balancing control of three-level active NPC converter using SHE-PWM," *IEEE Trans. Power Deliv.*, vol. 26, no. 1, Art. no. 1, Jan. 2011.
[24] T. Geyer, V. Spudić, W. van der Merwe, and E. Guidi, "Model predictive pulse pattern control of medium-voltage neutral-point-clamped inverter drives," in *IEEE Energy Conversion Congress and Exposition (ECCE)*, Sep. 2018, pp. 5047–5054.
[25] T. Geyer and V. Spudić, "Model predictive pulse pattern control with integrated balancing of the neutral point potential," in *21st European Conference on Power Electronics and Applications (EPE ECCE Europe)*, Sep. 2019, p. pp 1-10.
[26] B. Guan and S. Doki, "A current harmonic minimum PWM for three-level converters aiming at the low-frequency fluctuation minimum of neutral-point potential," *IEEE Trans. Ind. Electron.*, vol. 66, no. 5, pp. 3380–3390, May 2019.
[27] J. Chivite-Zabalza, P. Izurza-Moreno, D. Madariaga, G. Calvo, and M. A. Rodríguez, "Voltage balancing control in 3-level neutral-point clamped inverters using triangular carrier PWM modulation for FACTS applications," *IEEE Trans. Power Electron.*, vol. 28, no. 10, Art. no. 10, Oct. 2013.

Alain Sanchez-Ruiz (Senior Member, IEEE) received the B.Sc. degree in electronics engineering, the M.Sc. degree in automatics and industrial electronics, and the Ph.D. degree in electrical engineering from the University of Mondragon, Mondragon, Spain, in 2006, 2009, and 2014, respectively.
He joined Ingeteam R&D Europe, Zamudio, Spain, in May 2014, where he is currently an R&D Engineer. Since January 2017, he has also been a Lecturer with the University of the Basque Country (UPV/EHU), Bilbao, Spain. From February 2012 to May 2012 he was a Visiting Researcher at the University of Tennessee, Knoxville, TN, USA. His current research interests include modeling, modulation and control of power converters, multilevel topologies, advanced modulation techniques, high-power motor drives and grid-tied converters.

Mikel Mazuela was born in Irun, Spain, in 1986. He received the B.Sc. and M. Sc. Degrees in Electrical Engineering from the University of Mondragon, Mondragon, Spain, in 2007 and 2010 respectively. He obtained the Ph.D. degree in Electrical Engineering from the University of Mondragon in 2015.
He joined Ingeteam Power Technology in September 2015 where he worked as a R&D Engineer. He joined the Electronics Department of the University of Mondragon in 2016 as researcher and lecturer. His main research interests include power electronics, focusing mainly on modeling, modulation and control of power converters, multilevel topologies, advanced modulation techniques, DC-DC converters and Wide BandGap semiconductors.

Hector Fernandez-Rebolleda received the B.Sc. degree in industrial engineering and M.Sc. degree in industrial engineering from the University of Cantabria, Santander, Spain, and M.Sc. degree in industrial automation, electronics and control from the University of Deusto, Bilbao, Spain, in 2017, 2018, and 2019 respectively.
He joined Ingeteam Power Technology, Zamudio, Spain, in February 2019, where he is currently a Control & Regulation Engineer with the department of Marine & Industry. His current research interests include modulation, control of power converters, multilevel topologies, advanced modulation techniques, and high-power motor drives.

Salvador Ceballos received the M.S. degree in physics from the University of Cantabria, Santander, Spain, in 2001, and the M.S. and Ph.D. degrees in electronic engineering from the University of the Basque Country, Bilbao, Spain, in 2002 and 2008, respectively. Since 2002 he has been with Tecnalia Research and Innovation, where he is currently a principal researcher in the Energy and Environment Division. His research interests include multilevel converters for high and medium voltage applications, fault-tolerant power electronic topologies, renewable energy systems and power systems with high penetration of power converters.

Angel Perez-Basante received the B.Eng. degree in Telecommunications Engineering from the University of Valladolid, Spain, in 2006, the M.Eng. degree in Electronic Systems Engineering from the Technical University of Madrid (UPM), Madrid, Spain, in 2012 and the Ph.D. degree in Advanced Electronic Systems Engineering from the University of the Basque Country (UPV/EHU), Bilbao, Spain, in 2017. Currently, since March of 2017 he is working as a researcher with Tecnalia Research & Innovation in the Energy and Environment Division. From December 2012 to December 2016, he was a PhD student in the Applied Electronics Research Team (APERT) of the University of the Basque Country (UPV/EHU) in collaboration with Tecnalia Research & Innovation. From September 2015 to December 2015 he was a visiting researcher at the Chair of Power Electronics of the Christian Albrechts University, Kiel, Germany. His main research interests include multilevel converters, modulation and control strategies for power converters and renewable energy systems.

Irati Ibanez-Hidalgo was born in Bilbao, Spain, in 1996. She received the B.Sc. degree and the M.Sc. degree in industrial engineering from the University of the Basque Country (UPV/EHU), Bilbao, Spain, in 2018 and 2020 respectively. She is currently pursuing the Ph.D. project about the implementation in real time of low-frequency modulation techniques for high-power converters.
Since 2020, she has been with the Systems Engineering and Automation Department, University of the Basque Country (UPV/EHU), Spain, researching in the area of power electronics in collaboration with Tecnalia Research & Innovation, Derio, Spain and Ingeteam R&D Europe, Zamudio, Spain. Her research interests include modulation and control of power converters, multi-level converters and low-frequency modulation techniques.

Markel Zubiaga received the M.Sc. degree in electrical engineering in 2005 and the Ph. D. in 2011, both from the University of Mondragon, Spain. Since 2011, he has been working as R&D Engineer in the Renewable Energy Systems Department of Ingeteam.

His research interests are in the field of power electronics, renewable energy systems, energy transmission systems, power systems with high penetration of power converters and Grid Forming control.

Josep Pou (Fellow, IEEE) received the B.S., M.S., and Ph.D. degrees in electrical engineering from the Technical University of Catalonia (UPC)-Barcelona Tech, in 1989, 1996, and 2002, respectively.
In 1990, he joined the faculty of UPC as an Assistant Professor, where he became an Associate Professor in 1993. From February 2013 to August 2016, he was a Professor with the University of New South Wales (UNSW), Sydney, Australia. He is currently a Professor with the Nanyang Technological University (NTU), Singapore, where he is Cluster Director of Power Electronics at the Energy Research Institute at NTU (ERI@N) and co-Director of the Rolls-Royce at NTU Corporate Lab. From February 2001 to January 2002, and February 2005 to January 2006, he was a Researcher at the Center for Power Electronics Systems, Virginia Tech, Blacksburg. From January 2012 to January 2013, he was a Visiting Professor at the Australian Energy Research Institute, UNSW, Sydney. He has authored more than 380 published technical papers and has been involved in several industrial projects and educational programs in the fields of power electronics and systems. His research interests include modulation and control of power converters, multilevel converters, renewable energy, energy storage, power quality, HVdc transmission systems, and more-electrical aircraft and vessels.
He is Associate Editor of the IEEE Journal of Emerging and Selected Topics in Power Electronics. He was co-Editor-in-Chief and Associate Editor of the IEEE Transactions on Industrial Electronics. He received the 2018 IEEE Bimal Bose Award for Industrial Electronics Applications in Energy Systems.

Neha Beniwal (Student Member, IEEE) has received her B. Tech. degree in electrical engineering from National Institute of Technology, Kurukshetra, India in 2014 and her M. Tech. degree in power electronics, electrical machines & drives (PEEMD) from Indian Institute of Technology, Delhi in 2017. She joined the Ph.D. degree at the Interdisciplinary Graduate School, Nanyang Technological University, Singapore in 2017. She is currently working as Research Associate at the Energy Research Institute at Nanyang Technological University (ERI@N), Singapore. Her research interests include power electronics, renewable energy, microgrid, power quality, electrical machines and drives.
Ms. Beniwal is a recipient of POSOCO Power System Awards (PPSA) awarded by Power System Operation Corporation Ltd. (POSOCO) in association with Foundation for Innovation and Technology Transfer (FIIT), Indian Institute of Technology, Delhi in 2018. She is also the recipient of Prof. A.K. Sinha Cash Prize and IEEE-PEDES'96 Award at the Annual Convocation of Indian Institute of Technology, Delhi in 2017. She was also the vice-chair of the IEEE Joint IAS/PELS Student Branch Chapter, NUS during 2020-21.

Georgios Konstantinou (Senior Member, IEEE) received the B.Eng. degree in electrical and computer engineering from the Aristotle University of Thessaloniki, Thessaloniki, Greece, in 2007 and the Ph.D. degree in electrical engineering from UNSW Sydney (The University of New South Wales), Australia, in 2012. From 2013 to 2016, he was a Senior Research Associate with the University of New South Wales, Sydney, NSW, Australia, where he was part of the Australian Energy Research Institute. Since 2017, he has been with the School of Electrical Engineering and Telecommunications, UNSW Sydney, where he is currently a Senior Lecturer. His main research interests include multilevel converters, power electronics in HVDC, renewable energy and energy storage applications. He is an Associate Editor for IEEE Transactions on Power Electronics, IEEE Transactions on Industrial Electronics and IET Power Electronics.